224-Gb/s PDM-16-QAM Modulator and Receiver based on Silicon Photonic Integrated Circuits

Po Dong[1*], Xiang Liu[1], S. Chandrasekhar[1], Lawrence L. Buhl[1], Ricardo Aroca[2], Yves Baeyens[2], and Young-Kai Chen[2]

[1] *Bell Labs, Alcatel-Lucent, 791 Holmdel Road, Holmdel, NJ 07733, USA*

[2] *Bell Labs, Alcatel-Lucent, 600 Mountain Avenue, Murray Hill, NJ 07974, USA*

[*] *E-mail address: po.dong@alcatel-lucent.com*

Abstract: We demonstrate a coherent modulator and a receiver based on monolithically-integrated silicon photonic circuits, capable of modulating and detecting 224-Gb/s polarization-division-multiplexed 16-QAM. The high-degree photonic integration promises small-form-factor and low-power transceivers for future coherent systems.

OCIS codes: (250.5300) Photonic integrated circuits; (060.1660) Coherent communications; (130.0250) Optoelectronics.

1. Introduction

Optical coherent transmission is a key technology for high-capacity long-haul communications with channel data rates at 100 Gb/s and beyond [1]. Polarization-division-multiplexed quadrature phase-shift keying (PDM-QPSK) has been employed for current 100-Gb/s networks. Next-generation networks may utilize even higher modulation formats, such as 16-ary quadrature amplitude modulation (16-QAM). With its embedded high capacity, cost-effective electronic equalization of fiber impairments, and network monitoring capabilities, the coherent technology is also well-suited for metro networks. However, current coherent transceivers are implemented with discrete optical components which are bulky and expensive. Optical integration must be leveraged to solve this challenge.

Both InP and silicon photonic integrated circuits (PICs) are promising, each with their own merits and limitations. InP PICs can provide integrated lasers, but it is challenging to integrate lasers, modulators, photo detectors and polarization elements all on a single chip. Moreover, its yield and cost could be concerns. Silicon PICs take the advantage of CMOS foundries with large wafers, high yield and low cost. Silicon waveguides also have the flexibility to implement polarization combiners and rotators. With the emerging hybrid wafer-scale integration technology to bond InP on silicon [2], it is also feasible to support integrated amplifiers and lasers.

In this paper, we present a dual-polarization coherent modulator and a dual-polarization receiver based on silicon PICs. The main novelties are summarized as follows. First, the generation of 224-Gb/s Nyquist spectrally shaped (NSS) PDM-16-QAM signals is demonstrated, based on our previously reported PDM-QPSK modulator in Ref. [3]. Second, we implement a silicon coherent receiver by integrating on-chip polarization rotators (PRs) and splitters. Previously, silicon-based coherent receivers have been reported by using two-dimensional gratings which simultaneously serve as input couplers, polarization splitters and rotators [4]. However, these grating couplers suffer from limited optical bandwidths. We report here an edge-coupling scheme together with on-chip polarization elements to increase the bandwidth. Third, both the transmitter and receiver PICs were fabricated from the same process flow and they share the same polarization elements, allowing for future single-chip coherent transceivers.

2. Silicon PICs

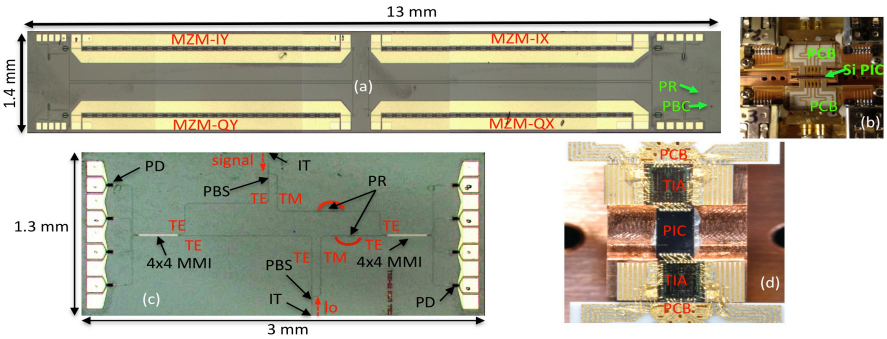

Fig. 1. (a) Photograph of the PIC for transmitter. MZM: Mach-Zehnder modulator; PR: polarization rotator; PBC: polarization beam combiner. (b) Photograph of the packaged PIC for transmitter. (c) Photograph of the PIC for receiver. PD: photo detector; IT: inverse taper; PBS: polarization beam splitter; MMI: multimode interference coupler. (d) Photograph of the packaged coherent receiver. PIC: photonic integrated circuit; TIA: transimpedance amplifier; PCB: printed circuit board.

The transmitter PIC integrates four single-drive push-pull silicon Mach-Zehnder modulators (MZMs), one PR and one polarization beam combiner (PBC), as shown in Fig. 1(a-b). Detailed information on this PIC can be found in [3]. The receiver PIC consists of two inverse tapers (ITs), two polarization beam splitters (PBSs), two PRs, two

multimode-interference coupler (MMI) 90-degree hybrids and eight germanium photodetectos (PDs). Fig. 1(c) shows the photograph of a fabricated PIC. Both PICs share the same design of PRs; PBC and PBS are identical. Refs. [5-7] have presented detailed device information. The overall chip sizes are 1.4 mm x 13 mm and 1.3 mm x 3 mm for the transmitter and receiver PICs, respectively.

The principle of operation of the receiver PIC is as follows. The optical signal enters the PIC from one facet with two polarizations. The optical local oscillator (LO) is coupled into the Si PIC from the other facet. Once coupled in, the signal and LO are divided into TE and TM polarizations by two PBSs. The TE polarized lights proceed to the 4x4 MMI-based 90-degree hybrids, whose four outputs are detected by four Ge PDs on the left side of the PIC (see Fig. 1(c)). The balance detection between the first and fourth PDs produces the in-phase TE-polarization components, and the second and third PDs produces the quadrature TE-polarization components. The TM components from the output of PBSs are converted to TE polarization by two PRs. The converted TE lights enter the right-side 4x4 MMI-based 90-degree hybrid, which is identical to that for the TE mode. The in-phase and quadrature in the TM-polarization components are produced with the same balance detection scheme as those for the TE mode.

These silicon PICs monolithically integrate silicon waveguides for routing and modulation, SiN waveguides for PRs, Ge waveguides for photo detection, and silica waveguides for input coupling. They were fabricated on a 200-mm silicon-on-insulator (SOI) wafer with a top silicon thickness of 220 nm. The fabrication sequences include silicon waveguide patterning and etching, SiN deposition and waveguide formation, various implantations and annealing to define modulator doping, germanium growth on silicon, and final metallization.

3. 224-Gb/s PDM-16-QAM generation

To generate coherent signals, a continuous-wave (CW) laser of 1539.77 nm was launched into the transmitter PIC in the TE mode. The four modulators were driven by four RF signals, generated by four 7-bit digital-analog-converters (DACs) and amplified by four RF amplifiers to a peak-to-peak voltage swing of ~5 V. Digital signal processing (DSP) was performed to form Nyquist pre-filtered driving signals with a roll-off factor of 0.1 to enable high spectral efficiency wavelength-division multiplexing [8]. The modulation speed was 28 Gbaud and the oversampling ratio was two, so the DACs were operating at 56 GSamples/s. The driving signals were modulated by pseudorandom bit sequence (PRBS) of length 2^{15}–1. Digital coherent detection was carried out by using a 50-GSamples/s digital sampling oscilloscope and offline DSP. We tested the performance of the transmitter PIC by using a commercial optical coherent receiver frontend.

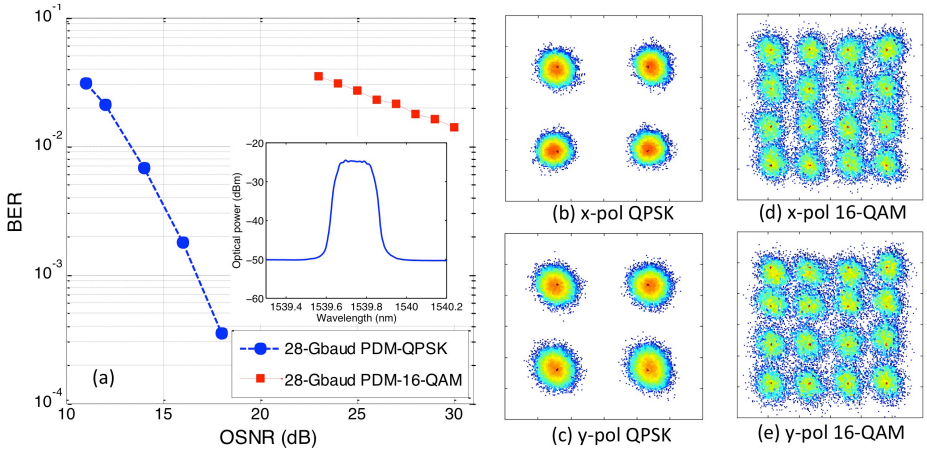

Fig. 2. 28-Gbaud PDM-QPSK and PDM-16-QAM generation using silicon PIC. (a): BER versus OSNR; (b) and (c): QPSK constellations; (d) and (e): 16-QAM constellations. Inset: the optical spectrum of the NSS PDM-16-QAM signal.

Figure 2 shows the performance of the generated PDM-QPSK and PDM-16-QAM signals. The recovered signal constellations in Fig. 2(b-e) show the successful signal generation, while the spectrum (inset) exhibits the Nyquist spectral shaping (NSS). The bit error ratio (BER), calculated by direct error counting, is shown as a function of optical signal-to-noise ratio (OSNR in both polarizations in 0.1 nm bandwidth) in Fig. 2(a). The required OSNR values at a BER of 2.4×10^{-2}, a typical threshold for soft-decision forward error coding (FEC) [9], are ~26 dB and ~12 dB for PDM-16-QAM and PDM-QPSK, respectively.

4. 28-Gbaud dual-polarization silicon coherent receiver

We characterized the receiver PIC prior to the packaging by measuring the PD performance. First, the dark currents of eight Ge PDs were collected and presented in Fig. 3(a). The dark currents for all the PDs are uniform and are ~180 nA at -1 V. Secondly, we measured the fiber-to-PD responsivities by launching the laser from a lensed fiber

into the chip. The total responsivity summed over eight PDs and averaged over two polarizations is shown in Fig. 3(b). The peak responsivity is ~0.3 A/W and the PIC's 1-dB responsivity bandwidth is measured as ~50 nm (1505 nm – 1555 nm), which is much larger than that of grating-based silicon receivers [4]. Finally, we measured the small-signal response of one of the eight PDs in the frequency region of 130 MHz to 20 GHz. Fig. 3(c) demonstrates that the PD's 3-dB bandwidth is >20 GHz with a reverse bias of 1 V. The silicon PIC was then wire-bonded to in-house SiGe TIAs (Fig. 1(d)), whose architecture was reported in Ref. [4].

We performed a system experiment of the packaged receiver by launching 112-Gb/s PDM-QPSK or 224-Gb/s PDM-16-QAM signals into the receiver. The signals were generated by either a commercial $LiNbO_3$ (LN) QPSK modulator or our silicon modulator. The receiver output from TIAs was directly connected to a real-time oscilloscope. Fig. 3(d-f) shows the results of coherent detection where the signals over two polarizations were well mixed before launching into the chip. Fig. 3(d) shows the measured BERs versus received OSNRs. In the case of QPSK signal generated by LN modulators without NSS, the required OSNR for a BER of 10^{-3} is ~15.3 dB, which is about 1-1.5 dB worse than a commercial coherent receiver. NSS signals have a penalty of ~1.6 dB in the PDM-QPSK cases (by comparing the red line with green line in Fig. 3(d)). Our silicon modulator has another 4-dB penalty at a BER of 10^{-3}, but lower penalty at higher BERs. For the NSS PDM-16-QAM signal generated by LN modulator, the BER floor is 9.4×10^{-3} at full OSNR, with the constellations shown in Fig. 3(e) and (f). The required OSNR is ~23 dB for a BER of 2.4×10^{-2}. Finally, for the NSS PDM-16-QAM signal generated by our silicon modulator, the BER floor is 4.8×10^{-2}, mainly caused by the silicon modulator performance, the use of NSS, and imperfect linear amplifiers. Although this high BER floor can be accommodated by large-overhead FEC [9], we expect the performance of the silicon modulator to be improved using the electrode design described in [7].

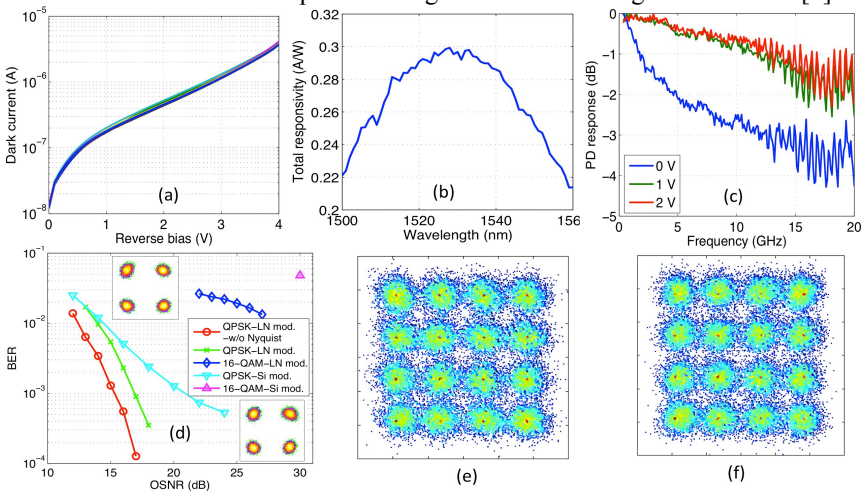

Fig. 3. Silicon coherent receiver. (a) Dark currents of eight Ge PDs. (b) Measured total fiber-to-PD responsivity. (c) Small-signal response of a Ge PD. (d) BER results of coherent detection of 112-Gb/s PDM-QPSK and 224-Gb/s PDM-16-QAM signals (insets show the constellations of PDM-QPSK for two polarizations). (e) and (f), X- and Y-constellations of PDM-16-QAM.

5. Conclusion

In conclusion, we have demonstrated monolithically integrated silicon PICs to generate and detect dual-polarization coherent signals. We achieved a record raw data rate of 224 Gb/s for a single carrier by silicon PICs. In the future, hybrid III-V/silicon lasers can be integrated on a common silicon platform, if a single-chip transceiver solution is desired. The high-degree photonic integration of this silicon-based transceiver platform may enable small form factors and low power consumption for future coherent transmission systems.

Acknowledgements: We thank T.-Y. Liow and G.-Q. Lo from the Institute of Microelectronics, Singapore for help in fabrication, D. Neilson, P. J. Winzer, and M. Zirngibl for support and J. Fernandes for assistance.

References

1. M. Berger, "100G Challenges and Solutions," in Market Watch Session, OFC/NOEC 2010.
2. A. Fang et al., "Electrically pumped hybrid AlGaInAs-silicon evanescent laser," Opt. Express **14**, 9203–9210 (2006).
3. P. Dong et al., "112-Gb/s monolithic PDM-QPSK modulator in silicon," ECOC 2012, paper Th.3.B.1.
4. C. R. Doerr et al., "Packaged monolithic silicon 112-Gb/s coherent receiver," IEEE Photon. Tech. Lett. **23**, 762–764 (2011).
5. L. Chen et al., "Monolithic silicon chip with 10 modulator channels at 25 Gbps and 100-GHz spacing," ECOC 2011, paper Th.13.A.1.
6. L. Chen et al., "Compact polarization rotator on silicon for polarization-diversified circuits," Opt. Lett. **36**, 469–471 (2011).
7. P. Dong et al., "High-speed low-voltage single-drive push-pull silicon Mach-Zehnder modulators," Opt. Express **20**, 6163–6169 (2012).
8. G. Bosco et al., "Performance limits of Nyquist-WDM and CO-OFDM in high-speed PM-QPSK systems," IEEE PTL **22**, 1129–1132 (2010).
9. L. Schmalen et al., "Combining spatially coupled LDPC codes with modulation and detection," Proc. ITG SCC, Munich (2013).